Collapse arrestors for deepwater pipelines Cross-over mechanisms

Rita G. Toscano, Luciano O. Mantovano, Pablo M. Amenta,
Roberto F. Charreau, Daniel H. Johnson, Andrea P. Assanelli
and Eduardo N. Dvorkin
Center for Industrial Research, TENARIS
Dr. Jorge A. Simini 250, Campana 2804, Argentina

Abstract

Using finite element models it is possible to determine the cross-over external pressure of different pipeline arrestor designs. In this paper these finite element models are discussed and validated by comparing their results with experimental determinations. The flipping and flattening cross-over mechanisms, that were previously described in the literature, are considered in the experimental validation of the numerical models.

1 Introduction

Deepwater pipelines are normally subjected to external pressure and bending and they are designed to prevent buckling and collapse failures. But a pipeline that is locally damaged may collapse and, if the hydrostatic pressure is high enough, the collapse may propagate along the pipeline. The collapse propagation pressure is the lowest pressure value that can sustain the collapse propagation [1]. Since the external collapse propagation pressure is quite low in comparison with the external collapse pressure, it is necessary to install buckle arrestors, at intervals along the pipeline, with the purpose of limiting the extent of damage to the pipeline by arresting the collapse propagation.

Buckle arrestors are devices that locally increase the bending stiffness of the pipe in the circumferential direction and therefore they provide an obstacle in the path of the propagating buckle; there are many different types of arrestors, but all of them typically take the form of thick-walled rings. The external pressure necessary for propagating the collapse pressure through the buckle arrestors is the collapse cross-over pressure.

In previous publications, CINI (Center for Industrial Research) presented finite element models that simulated the collapse and post-collapse behavior of steel pipes under external pressure and bending. Those finite element models were used to analyze the effect of different imperfections on the collapse and collapse propagation pressures of the steel pipes [2]-[7].

In this paper we focus on the analysis of the collapse and post-collapse behavior of pipelines reinforced with buckle arrestors: we develop finite element models to analyze the collapse, collapse propagation and cross-over pressures of reinforced pipes and we present an experimental validation of the models. In particular we consider the case of welded integral arrestors.

Two different integral buckle arrestor cross-over mechanisms were identified in the literature: flattening and flipping. The occurrence of either cross-over mechanism is determined by the geometry of the pipes and of the arrestors [8].

In the second section of this paper we describe our experimental facilities and the laboratory tests that we performed to determine, for different pipe - arrestor geometries, the collapse, propagation and cross-over pressures. In the third section we describe the finite element models that we developed to simulate the collapse tests and in the fourth section we compare the experimental and finite element results in order to validate the last ones.

Few experimental results are available in the literature for the cross-over of integral ring buckle arrestors under external pressure, on large diameter carbon steel pipes [8]-[14]. Therefore, this paper adds to the available technical literature in a range where more information can be useful.

2 Experimental results

2.1 Experimental set-up

The purpose of the laboratory tests developed for different combinations *[pipe + arrestor + pipe]* was to track the post-collapse equilibrium path for the assembly under external pressure and to determine from it the collapse and the cross-over pressure. For these tests we used the experimental set-up shown in Fig. (1).

Each sample had two pipes, one on each side of the arrestor, as described in Fig. (2). For each side, a L/D ratio greater than 7.5 was used in order to minimize the end - effects on the collapse loads. Two solid end-caps were welded on each end. The internal section of the end-caps was shaped to avoid localized failure during propagation (as observed on earlier tests). The shape of this section was derived from the finite element results of a free propagating buckle.

In Fig. (2) we present a detailed drawing and a photograph of the collapse chamber.

Each specimen was completely filled with water before the beginning of the test. From a hole in one of the end-caps the displaced water was directed to a container connected to a load cell. The load variation in the load cell is proportional to the displaced water and therefore to the variation of the specimen inner volume.

To localize the buckle initiation we milled a groove on one of the pipes (upstream pipe) as shown in Fig. (3)

In Fig. (4) we present a detail of the arrestors' geometry and we define the dimensions and steel grade[1] of the four tested samples.

During the tests, we continuously increased the external pressure as in a standard collapse test; after the collapse the pumping continued through the upstream propagation, cross-over of the arrestor and downstream propagation. All the test data was recorded at an average sampling rate close to 10Hz (see Fig. (5)).

2.2 Geometrical characterization of the tested samples

The outer surface of the samples was mapped using the shapemeter [2], as shown in Fig. (6); the corresponding Fourier decomposition of the outside surface for one of the tested samples is shown in Fig. (7). The zone with high amplitude corresponds to the milled groove, whereas the zone with low amplitude corresponds to the arrestor, which was machined in a lathe.

The thickness of the samples was also mapped using a standard ultrasonic gauge; the thickness map for the first sample is shown in Figs. (8) and (9).

2.3 Mechanical characterization of the tested samples

For all the pipe and arrestor materials we determined:

- Stress – strain curves (longitudinal tensile tests since the thickness of the pipes was too small for hoop samples).
- Hoop residual stresses (evaluated using slit ring tests).

In Table I we summarize the residual stress values.

Sample	$\frac{Measured \text{ max. Residual Stresses}}{Measured\ Yield\ Stress}$
1	0.39
2	0.47
3	0.47
4	0.49

Table I. Residual stresses measured using the slit ring test

3 The finite element model

Since the pipes that we analyze are in a *[diameter / thickness]* range suitable for being modeled using shell elements that incorporate shear deformations [2], we simulated the external pressure collapse test using the MITC4 [15]-[17] shell element implemented for finite elasto-plastic strains in the ADINA system [18].

[1] The steel Grade 6 defined by the standard ASTM A-333 has a minimum yield stress of 240 MPa and a minimum ultimate stress of 414 MPa.

The steel Grade X42 defined by the standard API-5L has a minimum yield stress of 290 MPa and a minimum ultimate stress of 414 MPa.

The numerical model was developed using a material and geometrical nonlinear formulation, which takes into account large displacements/rotations and finite strains [19], since it was shown in Ref. [4] that even tough the strains during post-collapse regime are rather small, at concentrated locations they can attain quite large values, as shown in Fig. (10). In previous publications we observed that when using an infinitesimal strains formulation we get results that have an excellent match with the experimental determinations; to confirm this assessment in this paper we compare the experimental results with the numerical results obtained under the assumption of infinitesimal strains and with the numerical results obtained under the assumption of finite strains.

The model incorporates the following features [19]:

- Von Mises elasto-plastic material model with isotropic multi-linear hardening. In Figs. (11) and (12) we show, for one of the tested samples, the experimental stress - strain curves and its fitting using a multilinear hardening model.
- Contact elements on the pipe inner surface in order to prevent its interpenetration in the post-collapse and propagation regimes.
- Nonlinear equilibrium path tracing via the algorithm developed in Ref. [20].
- Hoop residual stresses modeled with the technique discussed in Ref. [2].

In Fig. (13) we present the finite element mesh; in Fig. (14) we present a detail of the mesh in the pipes-arrestor transition which was modeled using variable thickness elements [19]; finally, in Fig. (15) we present a detail of the end-caps modeling; there are contact elements between the end-caps and the pipes.

4 Validation of the finite element results

In this section we discuss the validation of our finite element results by comparing them with experimental determinations that we obtained using the set-up described in the second section of this paper.

4.1 The finite element results

In order to explore the behavior of our finite element model, first we analyze two perfect samples, without residual stresses. In the first one we expect the collapse buckle to cross the arrestor with a flattening mode and in the second one with a flipping mode.

In each case we consider an imperfection, centered at a distance of $236.1mm$ from the upstream pipe end, with a shape [14]:

$$w_o(\theta) = -\Delta_o \left(\frac{D}{2}\right) \exp\left[-\beta \left(\frac{x}{D}\right)^2\right] \cos(2\theta) \tag{1}$$

where,

w_o : radial displacement;

θ : polar angle;

Δ_o : imperfection amplitude parameter (0.002);

β : parameter that decides the extent of the imperfection, in our case (2.32 D);

D : outside diameter;

x :axial coordinate.

In Fig. (16) we present the finite element predicted deformed shapes for a *[pipes – arrestor]* system exhibiting the flattening cross-over mechanism and in Fig. (17) we show the predicted deformed shapes for a system presenting the flipping cross-over mechanism.

In both cases we plot the external pressure as a function of the internal volume variation:

$$Vol.\,Variation = \frac{Vol.\,displaced\,water}{Original\,inside\,vol.} \tag{2}$$

Considering the [*external pressure-volume variation*] diagrams predicted by the finite element models, in each case we observe:

- The test starts at point "1" and while the external pressure grows the sample maintains its perfect shape and therefore there is a very small internal volume variation. Then the point of maximum pressure is reached ("collapse pressure") and the sample rapidly changes its cross-section shape; while the collapse buckle grows in its amplitude and extension in the upstream pipe axial direction, the external equilibrium pressure drops. At some point the collapse buckle extension starts to grow under constant external pressure ("collapse propagation pressure" [1]).

- At "2" opposite points located on the inner surface of the upstream pipe establish contact and afterwards, while the contact area extends, the external equilibrium pressure increases.

- While the collapse buckle in the upstream pipe approaches the arrestor the external equilibrium pressure keeps increasing but the downstream pipe does not collapse.

- At point "3" ("cross-over pressure") the collapse buckle crosses the arrestor and the downstream pipe collapses.

- Afterwards the collapse buckle propagates through the downstream pipe.

It is important to notice that in the case with the flattening cross-over mechanism the upstream and downstream pipe have their collapsed sections with the

same orientation while in the case with the flipping cross-over mechanism the collapse sections form an angle close to ninety degrees. It is also important to notice that the relation [*cross-over pressure / collapse pressure*] is much higher for the flipping case than for the flattening case.

4.2 Comparison between the finite element and experimental results

The four samples tested in the laboratory were modeled and the [*external pressure - volume variation*] equilibrium paths were determined.

In Table II we compare the FEM and experimental results.

Sample	$Col\ pres.: \frac{FEM-finite\ strains}{lab}$	$Cross-over\ press.: \frac{FEM-finite\ strains}{lab}$
1	0.924	1.004
2	0.928	0.985
3	0.951	0.926
4	0.852	0.883

Table II. Validation of the numerical results

It is important to point out that the finite element results indicated in this table were obtained considering that the residual stresses in the two pipe sections are the residual stresses measured in the full length pipe. The modifications in residual stresses induced by the pipe cutting, the welding and groove machining were not introduced in the model. The effect of the residual stresses on the collapse pressure was described by CINI in previous publications [2]-[7]. While this effect is quite important, we found with our numerical experimentation, that the effect of the residual stresses on the cross-over pressure is not so relevant, as shown by the model results that we present in Fig. (18).

In Figs. (19) and (20) we compare, for Samples 1 and 2 (flattening), the experimentally determined and FEM predicted equilibrium paths under the assumptions of finite strains and infinitesimal strains:

- During the laboratory determination for the first sample some water was spilled out of the measurement system, a fact that explains the shift observed, in the horizontal axis, between the FEM and experimental results.
- For the second sample the agreement between the FEM and experimental results is very good.
- The results obtained using FEM under the assumptions of finite and infinitesimal strains are very close.

In Fig. (21) we present, for Sample # 2, the deformed finite element mesh after cross-over.

In Figs. (22) and (23) we present the same comparison for Samples 3 and 4 (flipping). Again, the agreement between FEM and experimental results is very

good and again the results obtained using FEM under the assumptions of finite and infinitesimal strains are very close.

In Fig. (24) we present, for Sample # 4, the deformed finite element mesh after cross-over.

In Fig. (25) we present the contact pressure distribution in the third sample, immediately after the cross-over.

Finally in Fig. (26) we compare the experimentally observed and FEM predicted shapes for a case where the cross-over mechanism was flattening. In Fig. (27) we make the same comparison for a case in which the cross-over mechanism was flipping.

In both cases the agreement between numerical and experimental results is excellent.

It is interesting to notice that in Samples #2 and #4 the plastic strains in the deformed section knee are very high; in our case the elements were removed when the equivalent plastic strain reaches 100%; however more sophisticated criteria for the material damage can be implemented [21].

5 Conclusions

A 3D finite element model was developed in order to be able to analyze the behavior of an integral ring buckle arrestor crossed over by a propagating buckle. The model was validated by comparing the numerical predictions with experimental determinations.

The model is able to simulate both, the flipping and the flattening [8] cross-over mechanisms.

The agreement between the finite element predictions and the laboratory observations, both for the collapse and cross-over pressure, is very good; hence, finite element models can be used as a reliable engineering tool to assess the performance of integral ring buckle arrestors for steel pipes.

References

[1] A.C. Palmer and J.H. Martin, "Buckle propagation in submarine pipelines", *Nature*, **254**, pp. 46-48, 1975.

[2] A.P. Assanelli, R.G. Toscano, D.H. Johnson and E.N. Dvorkin, "Experimental / numerical analysis of the collapse behavior of steel pipes", *Engng. Computations*, **17**, pp.459-486, 2000.

[3] R.G. Toscano, P.M. Amenta and E.N. Dvorkin, "Enhancement of the collapse resistance of tubular products for deep-water pipeline applications", *Proceedings 25th. Offshore Pipeline Technology Conference, IBC*, Amsterdam, The Netherlands, 2002.

[4] R.G. Toscano, M. Gonzalez and E.N. Dvorkin, "Validation of a finite element model that simulates the behavior of steel pipes under external pressure", *The Journal of Pipeline Integrity*, **2**, pp.74-84, 2003.

[5] R.G. Toscano, C. Timms, E.N. Dvorkin and D. DeGeer, "Determination of the collapse and propagation pressure of ultra-deepwater pipelines", *Proceedings OMAE 2003 - 22nd. International Conference on Offshore Mechanics and Artic Engineering*, Cancun, Mexico, 2003.

[6] R.G. Toscano, M. Gonzalez and E.N. Dvorkin, "Experimental validation of a finite element model that simulates the collapse and post-collapse behavior of steel pipes", *Proceedings Second MIT Conference on Computational Fluid and Solid Mechanics*, (Ed. K.-J. Bathe), Elsevier, 2003.

[7] R.G. Toscano, L. Mantovano and E.N. Dvorkin, "On the numerical calculation of collapse and collapse propagation pressure of steel deep water pipelines under external pressure and bending: Experimental verification of the finite element results", *Proceedings 4th. International Conference On Pipeline Technology*, pp. 1417-1428, Ostend, Belgium, 2004.

[8] T.D. Park and S. Kyriakides, "On the performance of Integral Buckle Arrestors for Offshore Pipelines", *International Journal of Mechanical Sciences,* **39** pp.643-669, 1997.

[9] T.G. Johns, R.E. Mesloh and J.E. Sorenson, "Propagating buckle arrestors for offshore pipelines". *ASME Journal of Pressure Vessel Technology*, **100**, pp. 206-214, 1978.

[10] T.A. Netto and S.F. Estefen, "Buckle Arrestors for Deepwater Pipelines", *International Journal of Marine Structures*, **9**,pp.873-883, 1996.

[11] S. Kyriakides, T.D. Park and T.A. Netto, "On the design of Integral Buckle Arrestors for Offshore Pipelines", *International Journal of Applied Ocean Research*, **20,** pp.95-104, 1998.

[12] C.G. Langer, "Buckle arrestors for Deepwater Pipelines", *Proceedings of the Offshore Technology Conference, OTC 10711*, Houston, TX, U.S.A., 1999.

[13] T.A. Netto and S. Kyriakides, "Dynamic performance of integral buckle arrestors for offshore pipelines. Part I: Experiments", *International Journal of Mechanical Sciences*, **42**, pp.1405-1423, 2000.

[14] T.A. Netto and S. Kyriakides, "Dynamic performance of integral buckle arrestors for offshore pipelines. Part II: Analysis", *International Journal of Mechanical Sciences*, **42**,pp.1425-1452, 2000.

[15] E.N.Dvorkin and K.J.Bathe, "A continuum mechanics based four-node shell element for general nonlinear analysis", *Engng. Computations*, **1**, pp. 77-88, 1984.

[16] K.J.Bathe and E.N.Dvorkin, "A four-node plate bending element based on Mindlin / Reissner plate theory and a mixed interpolation", *Int. J. Numerical Methods in Engng.*, **21**, pp. 367-383, 1985.

[17] K.J.Bathe and E.N.Dvorkin, "A formulation of general shell elements - the use of mixed interpolation of tensorial components", *Int. J. Numerical Methods in Engng.*, **22**, pp.697-722, 1986.

[18] The ADINA SYSTEM, ADINA R&D, Watertown, MA, U.S.A.

[19] K.J. Bathe, *Finite Element Procedures*, Prentice Hall, NJ, 1996.

[20] K.J.Bathe and E.N.Dvorkin, "On the automatic solution of nonlinear finite element equations", *Computers & Structures*, **17**, pp. 871-879, 1983.

[21] Y. Bao and T. Wierzbicki, "A comparative study on various ductile crack formation criteria", *J. Engng. Materials and Technology ASME*, **126**, pp.314-324, 2004.

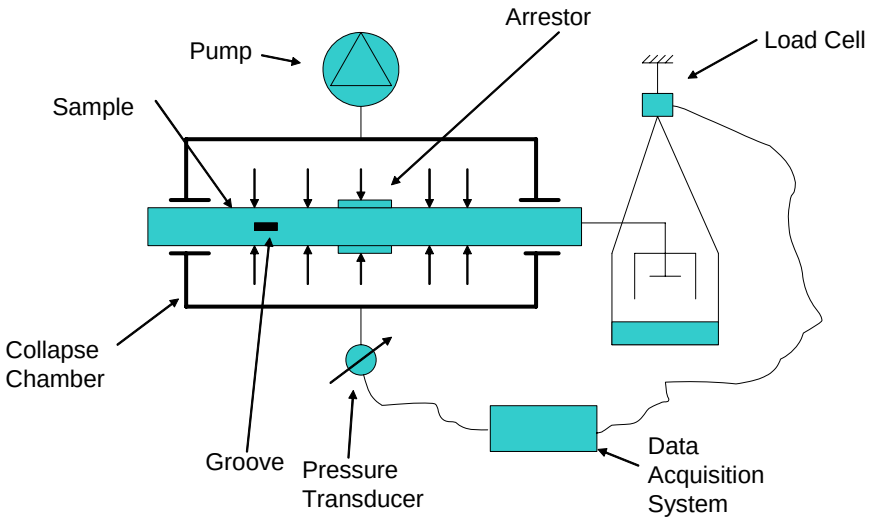

Figure 1: Experimental set-up

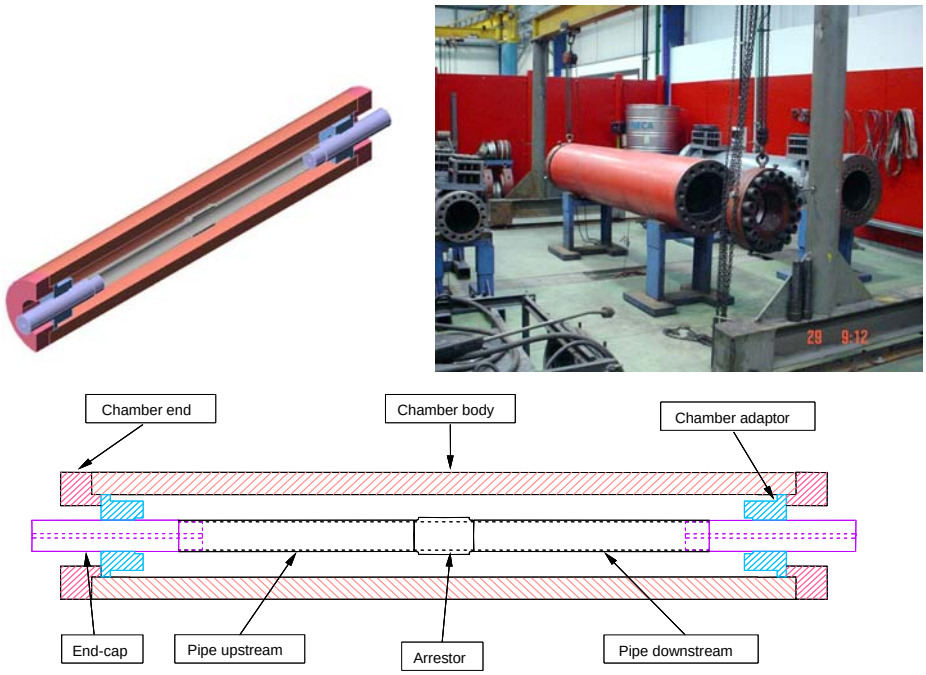

Figure 2: Collapse chamber

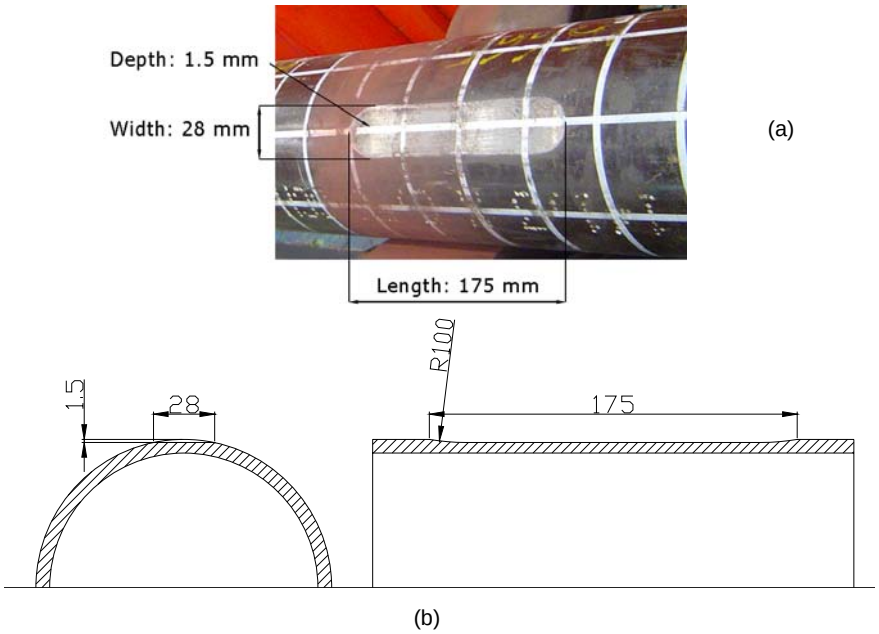

Figure 3: Groove machined on the upstream pipe to localize the collapse initiation. (a) General view (b) Detailed sections

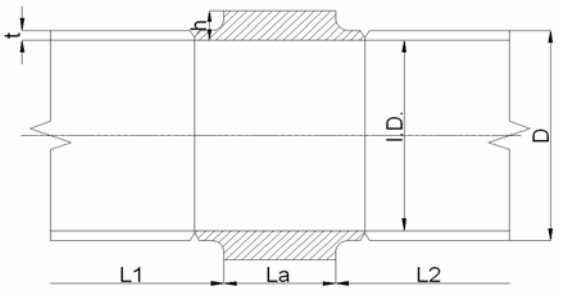

Sample	Pipe OD [mm]	Pipe thickness (t) [mm]	Pipe steel grade	Arrestor (h/t)	Arrestor (La/D)	Arrestor steel grade	Sample length [mm]	Expected cross-over mechanism
1	141.3	6.55	X42	2.0	0.50	6 (ASTM A-333)	2250	Flattening
2	141.3	6.55	X42	2.5	0.50	X42	2250	Flattening
3	141.3	6.55	X42	3.0	0.75	X42	2274	Flipping
4	141.3	6.55	X42	3.0	1.00	X42	2330	Flipping

Figure 4: Welded arrestors geometry and materials

Figure 5: Data acquisition during the collapse tests

Figure 6: The shapemeter [2]

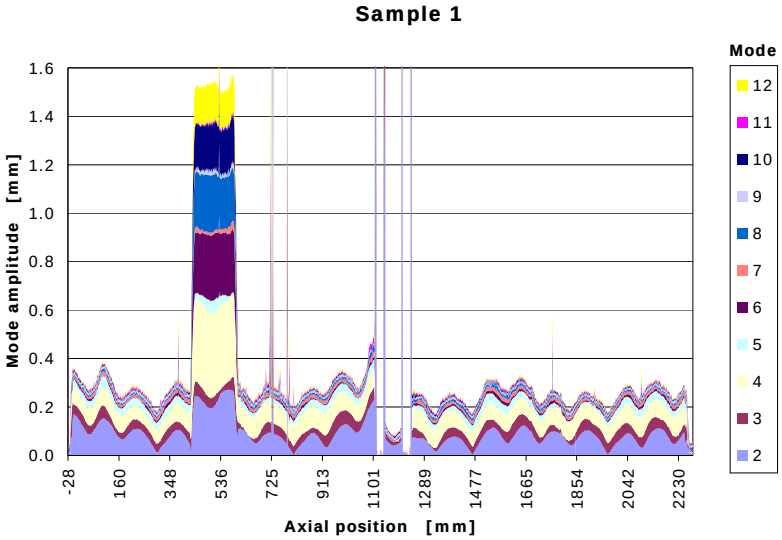

Figure 7: Outside surface Fourier decomposition for Sample # 1

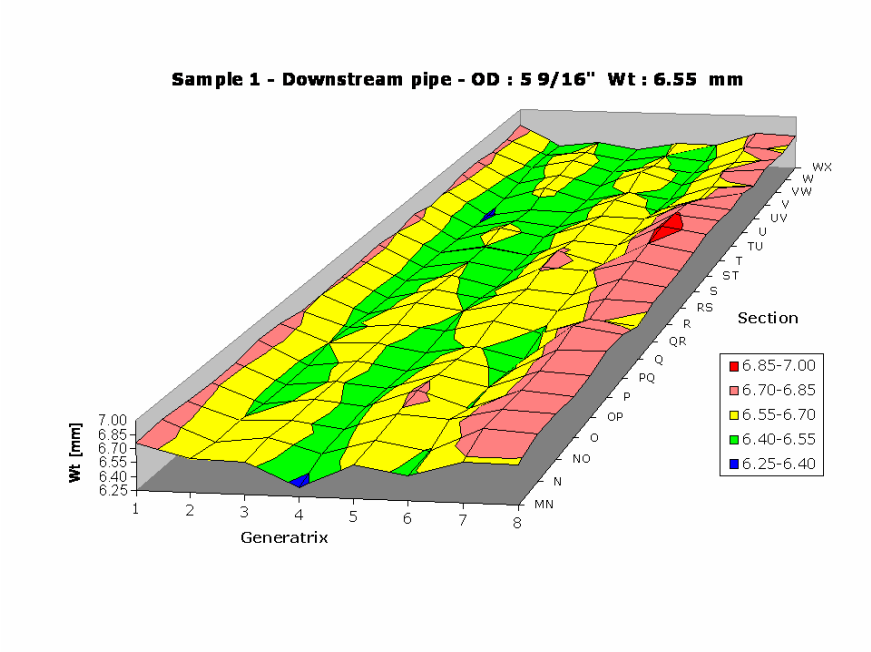

Figure 8: Sample # 1 - downstream pipe: thickness distribution

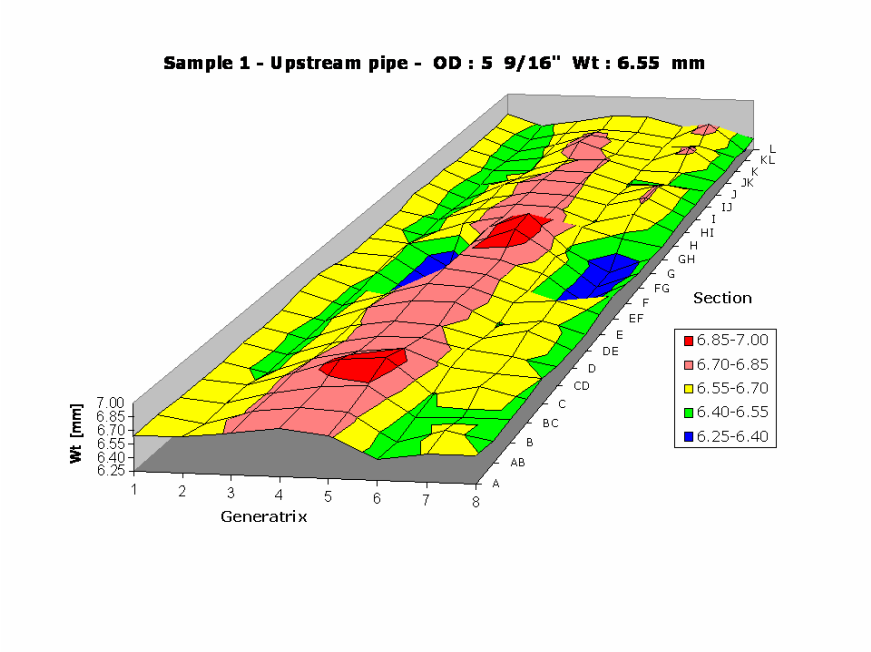

Figure 9: Sample # 1 - upstream pipe: thickness distribution

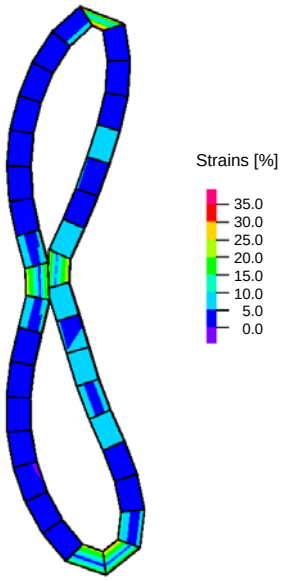

Figure 10: Typical post-collpase Hencky strains distribution

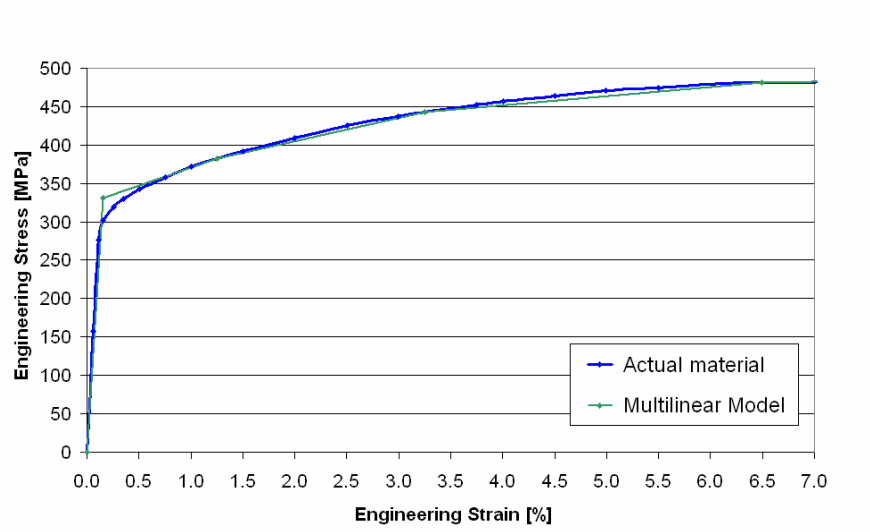

Figure 11: Material model for the pipe segments in sample # 1. Actual and numerical curves

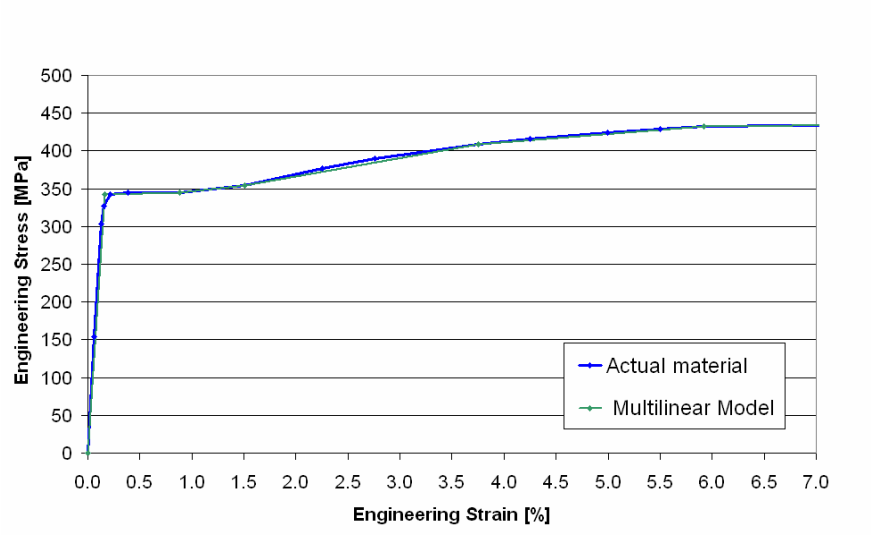

Figure 12: Material model for the arrestor in sample # 1. Actual and numerical curves

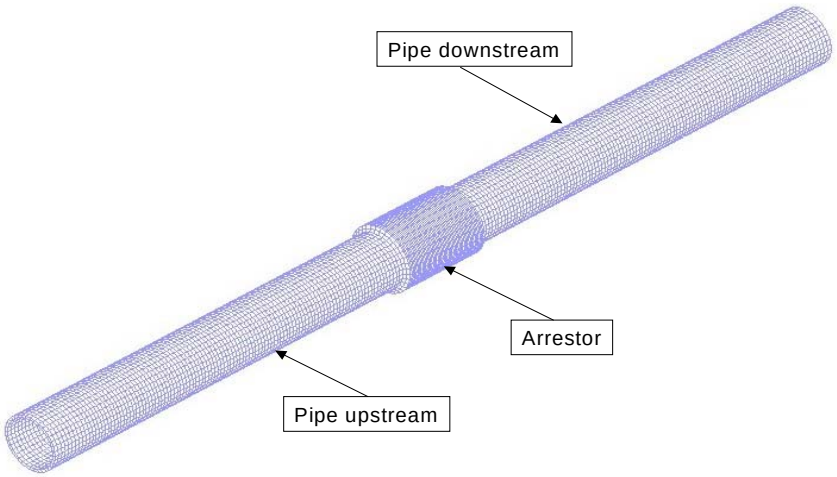

Figure 13: Finite element mesh (8500 elements and 42,500 d.o.f.)

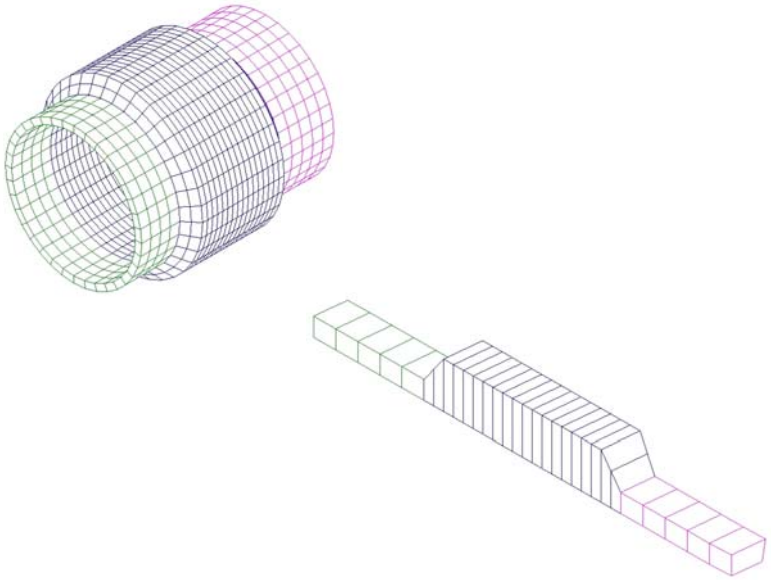

Figure 14: Modeling of the transition pipes-arrestor

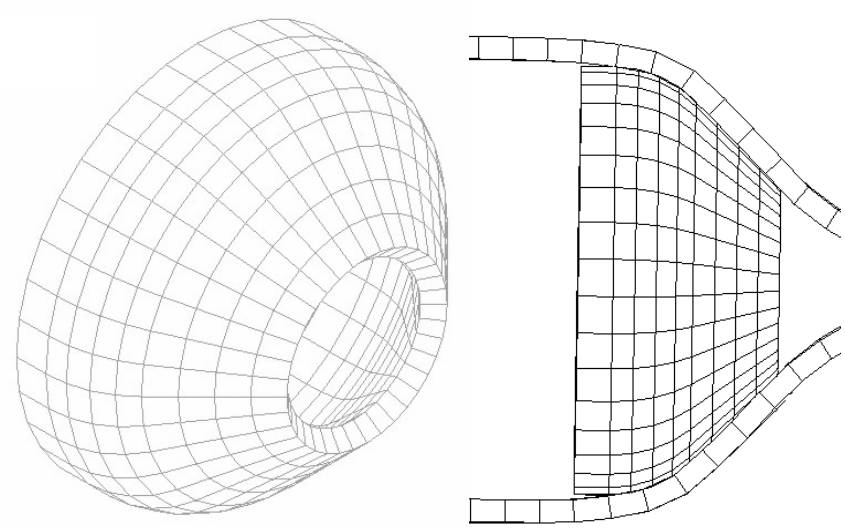

Figure 15: End-caps model

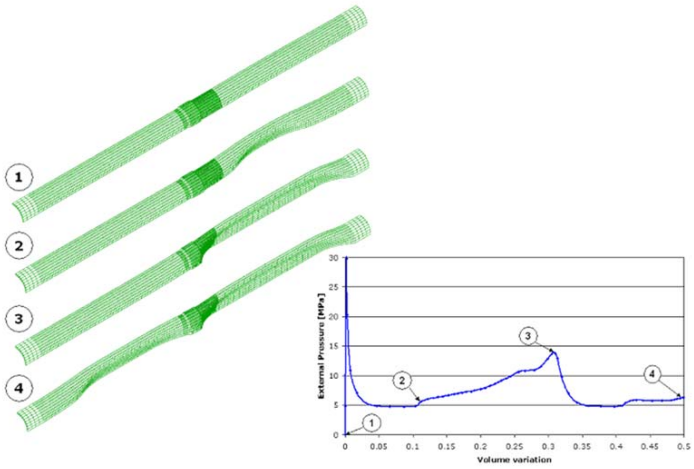

Figure 16: Finite element results for the case presenting a flattening cross-over

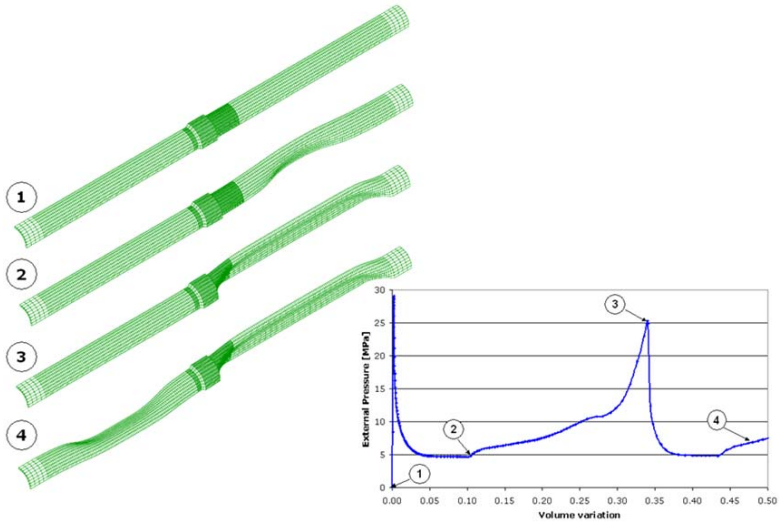

Figure 17: Finite element results for the case presenting a flipping cross-over

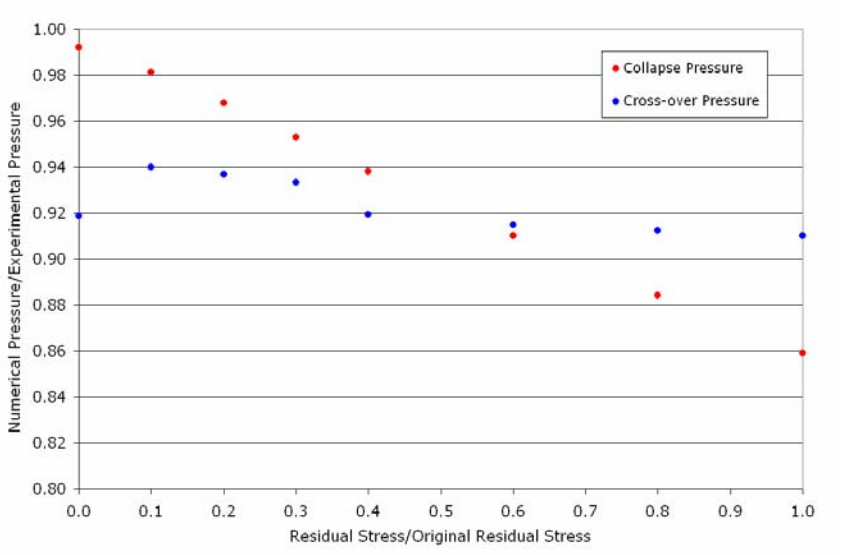

Figure 18: Residual stresses effect on the collapse and cross-over pressures (Sample # 4)

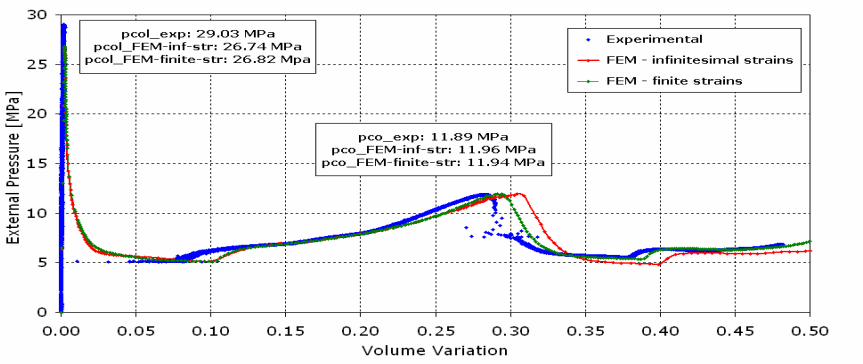

Figure 19: FEM vs. experimetal results for Sample # 1 (flattening cross-over)

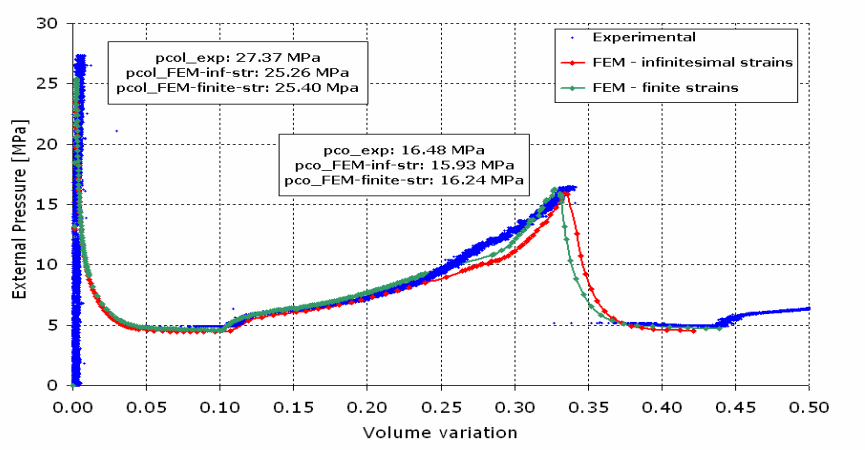

Figure 20: FEM vs. experimetal results for Sample # 2 (flattening cross-over)

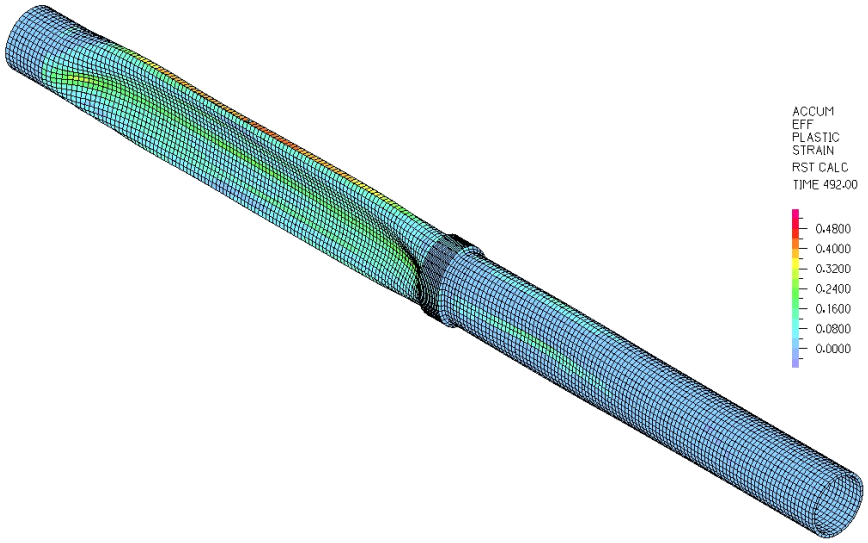

Figure 21: Deformed mesh for Sample # 2 (flattening). The accumulated effective plastic strains are shown.

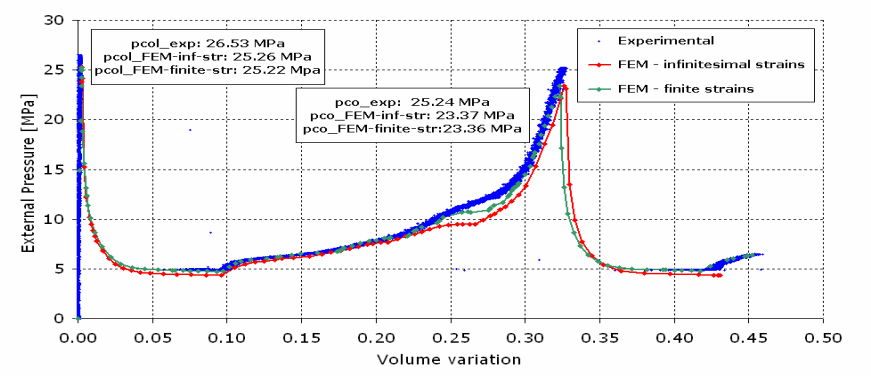

Figure 22: FEM vs. experimetal results for Sample # 3 (flipping cross-over)

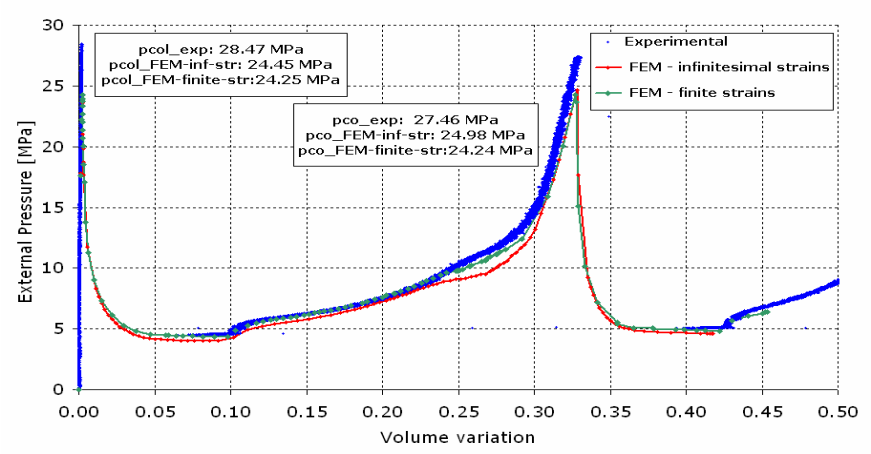

Figure 23: FEM vs. experimetal results for Sample # 4 (flipping cross-over)

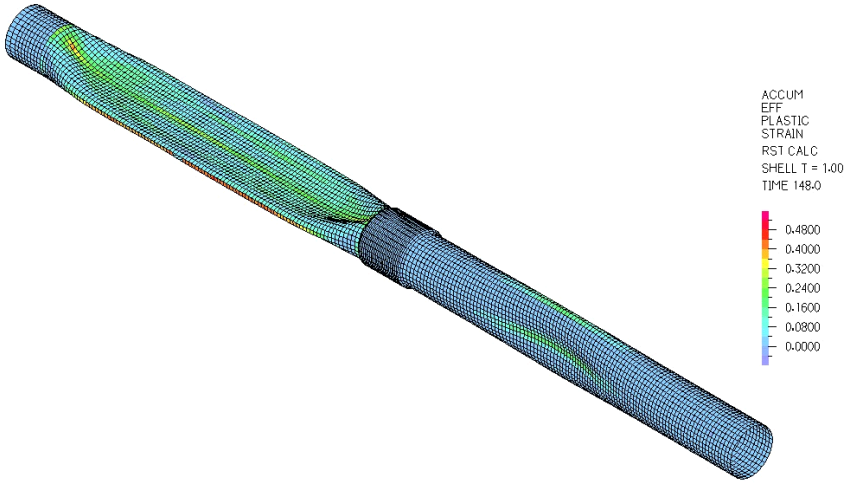

Figure 24: Deformed mesh for Sample # 4 (flipping). The accumulated effective plastic strains are shown.

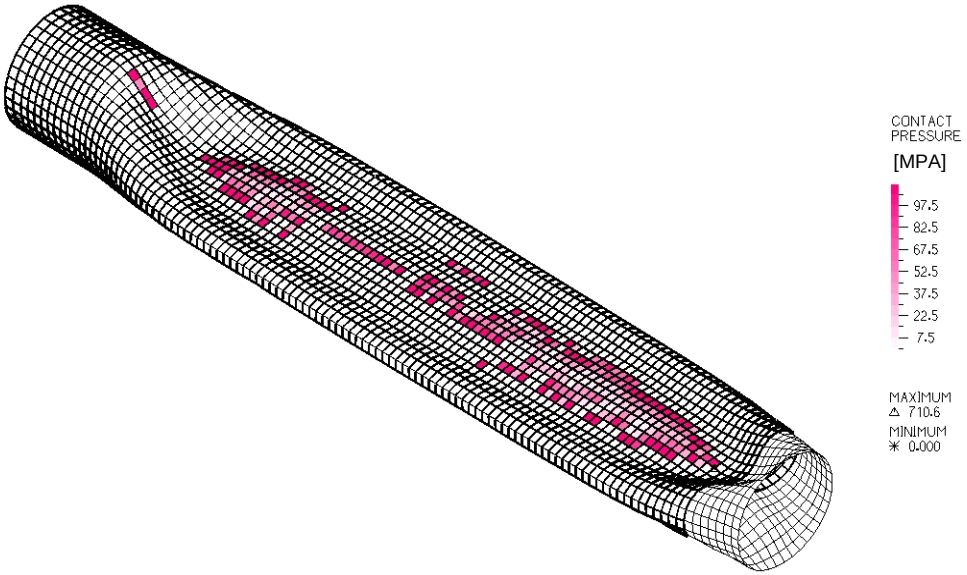

Figure 25: Contact pressure distribution in the upstream pipe of sample # 3 after cross-over

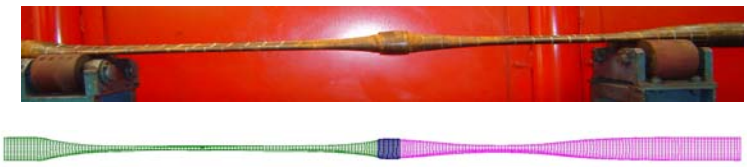

Figure 26: Experimentally observed and FEM predicted shapes of collapsed pipes after a flattening cross-over (Sample # 2)

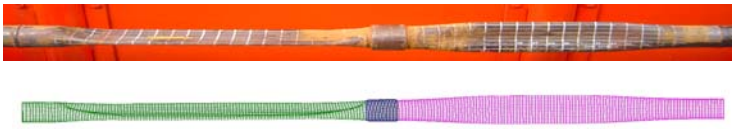

Figure 27: Experimentally observed and FEM predicted shapes of collapsed pipes after a flipping cross-over (Sample # 3)